HHS Public Access

Author manuscript

Biomed Mater. Author manuscript; available in PMC 2021 August 31.

Published in final edited form as:

Biomed Mater. ; 15(5): 055035. doi:10.1088/1748-605X/ab9bb0.

Concurrent multi-lineage differentiation of mesenchymal stem cells through spatial presentation of growth factors

Amelia Hurley-Novatny[1,2], **Navein Arumugasaamy**[1,2], **Megan Kimicata**[2,3], **Hannah Baker**[1,2], **Antonios G Mikos**[2,4], **John P Fisher**[1,2]

[1]Fischell Department of Bioengineering, University of Maryland, College Park, MD 20742, United States of America

[2]Center for Engineering Complex Tissues, University of Maryland and Rice University, College Park, MD 20742, United States of America

[3]Department of Materials Science and Engineering, University of Maryland, College Park, MD 20742, United States of America

[4]Department of Bioengineering, Rice University, Houston, TX 77030, United States of America

Abstract

Severe tendon and ligament injuries are estimated to affect between 300 000 and 400 000 people annually. Surgical repairs of these injuries often have poor long-term clinical outcomes because of resection of the interfacial tissue—the enthesis—and subsequent stress concentration at the attachment site. A healthy enthesis consists of distinct regions of bone, fibrocartilage, and tendon, each with distinct cell types, extracellular matrix components, and architecture, which are important for tissue function. Tissue engineering, which has been proposed as a potential strategy for replacing this tissue, is currently limited by its inability to differentiate multiple lineages of cells from a single stem cell population within a single engineered construct. In this study, we develop a multi-phasic gelatin methacrylate hydrogel construct system for spatial presentation of proteins, which is then validated for multi-lineage differentiation towards the cell types of the bone-tendon enthesis. This study determines growth factor concentrations for differentiation of mesenchymal stem cells towards osteoblasts, chondrocytes/fibrochondrocytes, and tenocytes, which maintain similar differentiation profiles in 3D hydrogel culture as assessed by qPCR and immunofluorescence staining. Finally, it is shown that this method is able to guide heterogeneous and spatially confined changes in mesenchymal stem cell genes and protein expressions with the tendency to result in osteoblast-, fibrochondrocyte-, and tenocyte-like expression profiles. Overall, we demonstrate the utility of the culture technique for engineering other musculoskeletal tissue interfaces and provide a biochemical approach for recapitulating the bone-tendon enthesis *in vitro*.

Keywords

mesenchymal stem cells; bone-tendon enthesis; orthopaedic tissue engineering; interfacial tissue engineering; transforming growth factor β; differentiation

jpfisher@umd.edu.

1. Introduction

Severe tendon tears, which can result from trauma, overuse, or sports injuries, affect between 300 000 and 400 000 people annually [1]. Due to the avascular nature of the tendon, these injuries do not heal on their own, and therefore often require surgical intervention [1, 2]. Surgery, which typically involves directly anchoring the tendon to the bone using sutures or screws, fails in 25%–35% of patients [3, 6]. This failure can be partially attributed to resection of the bone-tendon enthesis during surgery [7]. An intact enthesis transfers tensile, compressive, and shear stresses between the tendon and bone through its complex, heterogeneous structure [8, 9]. Following surgery, this critical region of tissue becomes replaced with disorganized, fibrotic scar tissue, which results in stress concentration and ineffective stress transfer [7, 10]. Therefore, it is critically necessary to explore alternative methods to redevelop the enthesis following surgery. Tissue engineering is a potential strategy to fill this need because it has potential for engineering complex, heterogeneous tissues.

The enthesis consists of four regions, the subchondral bone, mineralized fibrocartilage, un-mineralized fibrocartilage, and the tendon, each with distinct mechanical properties determined by the extracellular matrix (ECM). The structure of the ECM is regulated by the cell types within each region, which are osteoblasts, fibrochondrocytes, and tenocytes, respectively [11]. Thus, their relative spatial localization is integral to the foundation of a tissue-engineered construct. While fabricating a construct using primary cells appears to be a logical choice, use of these cells is limited by lack of donor tissue and poor proliferation [12, 13]. Mesenchymal stem cells (MSCs), however, are easily sourced from a variety of adult tissues, are more proliferative than terminally differentiated cells, and can be differentiated into multiple musculoskeletal cell lineages, including those of the enthesis [14, 16]. Concurrent differentiation of stem cells towards the lineages within the enthesis within a single 3D construct would be less time-intensive than differentiating the cell populations individually, and could encourage important cell–cell communication during differentiation [17]. When starting with a single population of MSCs, biochemical cues to induce differentiation towards multiple lineages must be presented within the construct with spatial specificity [18]. Transforming growth factor β (TGFβ) family proteins play an integral role in development of the enthesis *in utero*, and have been used to induce differentiation of MSCs towards the multiple cell types of the enthesis *in vitro* [19, 21]. It has previously been shown that gelatin methacrylate (GelMA) can electrostatically bind TGFβ family growth factors and support MSC viability and differentiation [22, 25], making it a useful biomaterial for this application. Additionally, given that GelMA can be thermally cured before it is photocrosslinked, it can be 3D printed or cast to have distinct regions [26, 27]. Thus, it was hypothesized that GelMA could be used for spatial presentation of growth factors to generate a multi-phasic construct.

This study develops a GelMA hydrogel construct with spatial control of growth factors to induce multi-lineage differentiation of MSCs. This paper sought to (1) fabricate a GelMA construct with spatial specificity, (2) assess the differentiation of MSCs in response to TGFβ family growth factors, and (3) assess regional MSC phenotype in response to spatially distinct growth factor concentrations. To achieve these ends, the GelMA constructs were

fabricated using sequential layering of hydrogel precursor solutions and validated for spatial loading using fluorescently tagged proteins. This fabrication method was then assessed for the ability to induce spatially distinct MSC differentiation. Bone morphogenetic protein (BMP) 4, BMP12, and TGFβ3 were evaluated for their effect on MSC expression of protein and genetic markers of osteogenic, chondrogenic, and tenogenic differentiation. The growth factor dosages which induced the highest up-regulation of osteogenic, chondrogenic, and tenogenic marker gene expression and greatest extent of tissue-specific protein deposition within both the 2D and 3D environments were spatially loaded into a GelMA hydrogel continuously seeded with MSCs, with the hypothesis that the MSC phenotypic response would vary within the multi-phasic construct. The results of this study indicate that the fabrication method developed is able to generate a construct for spatial presentation of growth factors. Furthermore, MSCs have spatial differences in phenotype when seeded within the patterned construct. This work presents a system to engineer musculoskeletal interfacial tissues and further the understanding of concurrent differentiation characteristics of MSCs with spatial presentation of multiple growth factors. To the best of the authors' knowledge, this is the first use of GelMA for presentation of growth factors with a complex spatial pattern.

2. Methods

2.1. Cell culture

Human bone marrow MSCs were grown in basal growth medium from Rooster Bio (Rooster Bio, Fre-derick, MD). MSCs were used for assays at passage 5. 2D studies were conducted in well plates (CellTreat, Pepperell, MA) seeded with 10 000 cells cm^{-2}. Cell-laden GelMA constructs were cultured in non-tissue culture treated 24 well plates (CellTreat) to limit cell adhesion onto the plate. Differentiation media consisted of 10% fetal bovine serum (FBS) and 1% Antibiotic/Antifungal in Dulbecco's Minimum Essential Medium (DMEM) (Gibco, USA). Treated groups included solubilized BMP4 (Gibco), TGFβ3 (Gibco), or BMP12 (Fitzgerald Industries International, Acton, MA) at various concentrations, as discussed below. All studies included a group without solubilized growth factors as a negative control.

2.2. Synthesis of GelMA

GelMA was synthesized in a similar fashion to that described by Kuo *et al* [28]. Briefly, type A gelatin (Sigma Aldrich, USA), bloom strength 300, was dissolved in phosphate buffered saline (PBS) and reacted with methacrylic anhydride at 50 ℃ for 2 h, diluted 1:1 in PBS, and dialyzed for 3 d at 50 ℃ using a 10 000 Da cutoff dialysis membrane (Thermo Scientific Pierce, USA). It was subsequently lyophilized, and this product was stored at −80 ℃ until use. Generation of 3D constructs from this material is described below.

2.3. Fabrication of multi-phasic 3D constructs

GelMA hydrogels were fabricated using a precursor solution of 8% w/v lyophilized GelMA, 2% w/v gelatin, and 0.2% w/v Irgacure 2959 (IGM Res-ins) in PBS, which was allowed to dissolve at 50 °C for 30 min with stirring. For cell-laden constructs, MSCs were lifted and re-suspended in GelMA at a concentration of 3 million cells ml^{-1}. Negative controls had no added growth factors. Non-multiphasic single growth factor constructs contained either 12.5

ng ml^{-1} BMP4, 200 ng ml^{-1} BMP4, or 10 ng ml^{-1} TGFβ3 added into the precursor solution. These same solutions were used to create the spatially controlled gels with the fabrication method described below. Gels were photocrosslinked and cultured in differentiation medium with 50 μg/mL ascorbic acid to promote protein deposition [29]. Multilayer constructs were fabricated as described below.

Constructs were created in a cylindrical mold created using a 3D printed E-Shell component and an acrylic backing. The E-Shell component was produced via stereolithography on a Perfactory printer (EnvisionTec, Dearborn, MI) using their proprietary E-Shell 300 material (EnvisionTec). The E-Shell component contained holes of 6 mm diameter and 7 mm depth (schematic in figure 1(a)). Molds were completed by binder-clipping an acrylic sheet to one side of the E-Shell component. Gels were cooled for 10 min per layer at room temperature to allow solidification. Constructs were UV crosslinked for 3 min on each side at 2.0 mW cm^{-2} (UVP) following addition of all layers of hydrogel precursor.

To assess the ability to fabricate multi-phasic constructs, distinct regions containing fluorescently tagged bovine serum albumin (BSA) were developed by sequential layering of hydrogel precursor, thermal gelation at room temperature between layers, and UV crosslinking after the construct was completely cast, as outlined in figure 1(b). Table 1 and figure 1(b) demonstrate how this was carried out. Briefly, hydrogel precursor solution was layered with thermal gelation between layers. Stepped gradients were generated by decreasing the growth factor concentration by 25% with each layer. Constructs containing varying concentrations of FITC- and Texas Red-conjugated BSA were imaged on a fluorescent microscope (Nikon, Japan) immediately after crosslinking for 2 min on each side. Quantification of fluorescent intensity along the length of the construct was conducted using the linear intensity function in FIJI [30]. Quantification of the overlap of FITC and Texas Red channels was conducted in FIJI by thresholding for positive staining, then calculating the length of that overlap, and normalizing to the total construct length. Constructs containing cells and growth factors were fabricated in an identical fashion, except for the use of BMP4 or TGFβ3 instead of BSA, and the inclusion of MSCs.

2.4. Quantification of gene expression via qPCR

Cells encapsulated in GelMA were isolated using an enzymatic protocol by incubating scaffolds, which were mechanically disrupted with scissors, in 4 mg ml^{-1} Papain enzyme (Sigma-Aldrich, St. Louis, MO) at 37 ℃ for 1 h, vortexing the solution every 5 min. Multi-phasic constructs were cut into thirds perpendicular to the cylindrical axis, and each third was digested separately. The suspension of dissolved GelMA and cells was centrifuged at 1000×g for 5 min to pellet the cells. The super-natant was removed and the pellet was lysed with TRIzol (Qiagen, Germany). Cells in the monolayer were lysed with TRIzol in the well plate. RNA extraction was performed using a modified Qiagen protocol as described in previous studies [31]. Briefly, cells were lysed using TRIzol, DNA was precipitated using chloroform, and the aqueous portion was removed for RNA extraction and purification using a Qiagen RNAeasy kit (Qiagen). The Qiagen RNAeasy kit protocol was followed as supplied by Qiagen. cDNA was synthesized using the High-Capacity cDNA Archive Kit (Applied Biosystems, Waltham, MA) in manufacturer-specified ratios and thermo-cycling

the mixture for 10 min at 25 ℃, 120 min at 37 ℃, and 5 min at 85 ℃. The cDNA was stored at −20 ℃ until further use. qPCR was performed on cDNA using a AB7900HT RT-PCR machine (Applied Biosystems) using FAM-reporter probes (Thermo Fisher) and PCR Mastermix (Thermo Fisher). Probes for GAPDH, *RUNX2*, osteopontin (*SPP1*), *SOX9*, aggrecan (*ACAN*), Scleraxis (*SCX*), and tenomodulin (*TNMD*) were purchased from Thermo Fisher. Relative expression is reported as $2^{(-\Delta\Delta CT)}$. Confidence intervals are reported as $2^{(-\Delta\Delta CT \pm SD)}$ [32].

2.5. Immunofluorescence staining

Constructs were fixed in 4% paraformaldehyde (Sigma), 1% sucrose (Sigma) in PBS. After washing with PBS, constructs were blocked using 5% v/v goat serum and 1% w/v BSA in PBS for 1 h, then incubated with mouse-anti-collagen I antibody (1:500, Abcam), mouse-anti-aggrecan (1:500, Novus Biologicals, Centennial, CO), or mouse-anti-osteopontin (1:250, Abcam). Secondary staining was done immediately after each primary antibody using goat-anti-mouse antibody conjugated with Alexa Fluor 488 (1:500, Invitrogen). A second set of primary antibodies was incubated with rabbit-anti-collagen II (1:200, Abcam), rabbit-anti-decorin (1:100, Abcam), or rabbit-anti-tenomodulin (1:200, Abcam) overnight. They were then secondary stained with goat-anti-rabbit antibody conjugated with Alexa Fluor 594 (Invitrogen) following the manufacturer's instructions. Following the final secondary stain, nuclei were counter-stained with DAPI. PBS washes were done between each antibody solution change. Fluorescent images were taken on a Nikon Eclipse Ti2 Series microscope and confocal images were taken on an Olympus FV3000. Multi-phasic constructs had images taken in three distinct regions. Image processing and analysis were done using FIJI software [30].

2.6. Statistical analysis

Statistics are reported as mean ± one standard deviation. The sample size was $n = 3$ experimental replicates, unless otherwise stated. Comparisons were made using ANOVA with Tukey's post-hoc test. Statistical significance was considered as $p < 0.05$.

3. Results

3.1. Protein localization immediately following fabrication of hydrogel

The fabrication method, described above and outlined in figure 1(b), was assessed for its ability to create a multi-phasic construct. Fluorescent images were taken of the multi-phasic hydrogels fabricated with multiple layers of hydrogel precursor containing differing concentrations of FITC- and Texas Red-conjugated BSA. As demonstrated in figure 1(d), the images demonstrate that fluorescent proteins were localized to the region in which they were cast in the biphasic hydrogel (schematic in figure 1(c)). Quantification along the length of the hydrogel, shown in figure 1(e), confirms this localization by indicating a peak in FITC fluorescence and Texas Red fluorescence in the regions cast with those fluorescent proteins, respectively. When casting a multi-phasic construct with an inverse gradient, as described in table 1, visual inspection shows a construct with greater overlap of FITC and Texas Red protein fluorescence (figure 1(g)). Quantification of fluorescent intensity, which is representative of the width of the construct, shows greater overlap of FITC and Texas Red

fluorescence than in the biphasic group (figure 1(h)). Furthermore, quantification of the overlap, shown as percentage of overlap compared to total construct length, demonstrates a positive FITC-Texas Red overlap of 19% in the distinct phases group (figure 1(e)) and 68% overlap in the gradient group (figure 1(h)).

3.2. MSCs respond differentially to TGFβ-family growth factors

MSCs were cultured in the presence of different concentrations of BMP4, TGFβ3, and BMP12, then analysed by qPCR and immunofluorescence to assess differentiation towards osteogenic, chondrogenic, and tenogenic lineages, as well as evaluate the compatibility of the basal medium with differentiation towards these three lineages. We assayed for early markers of differentiation *RUNX2, SOX9*, and *SCX. RUNX2*, an osteogenic marker, was slightly up-regulated in response to 12.5 ng ml^{-1} BMP4 and all concentrations of TGFβ3 after 7 d (figure 2(a)). Expression of *SOX9*, a chondrogenic marker, was up-regulated 4.8-fold after 3 d and 4.1-fold after 7 d in response to 10 ng ml^{-1} TGFβ3 (figure 2(b)). Additionally, expression was slightly increased in all experimental groups at 7 d except 25 ng ml^{-1} BMP4 and 200 ng ml^{-1} BMP12. *SCX* expression was highest following treatment with 10 ng ml^{-1} TGFβ3 at both 3 and 7 d, while also being slightly up-regulated at 3 d following treatment with 2.5 ng ml^{-1} and 40 ng ml^{-1} TGFβ3 (figure 2(c)). Expression of *SPP1, ACAN*, and *TNMD* were assessed as late markers of osteogenesis, chondrogenesis, and tenogenesis, respectively. *SPP1* expression was increased in response to 10 ng ml^{-1} TGFβ3 treatment (figure 2(d)). *ACAN* expression was significantly up-regulated in response to 25 ng ml^{-1} BMP4 (5.7-fold, $p < 0.0001$) and 200 ng ml^{-1} BMP4 (55.6-fold, $p < 0.0001$) (figure 2(e)). After 7 d, cells treated with 10 ng ml^{-1} TGFβ3 had significantly up-regulated *TNMD* expression ($p < 0.05$) (figure 2(f)).

Immunofluorescence staining for key structural proteins collagen I and collagen II, as well as proteoglycans aggrecan and decorin, was conducted to provide further evidence for differentiation. Concurrent expression of collagen I and decorin is indicative of osteogenesis or tenogenesis, and expression of collagen II and aggrecan is indicative of chondrogenesis. Cells treated with BMP4 showed higher deposition of collagen I than collagen II, and more collagen I than the no growth factor control and TGFβ3 groups (figure 2(g)). Collagen II was expressed by the no growth factor control and TGFβ3-treated group (figure 2(g)). Decorin was highly deposited following treatment with 12.5 ng ml^{-1} BMP4 (figure 2(h)). The remainder of the groups expressed a mixture of aggrecan and decorin, with most positive aggrecan staining being found in the TGFβ3 treatment group. Increases in expression in all six genetic and all four protein markers evaluated compared to no growth factor control indicate that the basal differentiation medium is compatible with differentiation towards the three intended lineages.

Based on the results obtained during 2D MSC culture, the effects of 12.5 ng ml^{-1} BMP4, 200 ng ml^{-1} BMP4, and 10 ng ml^{-1} TGFβ3 on MSC differentiation in 3D were assessed. *RUNX2* expression was slightly decreased in response to 200 ng ml^{-1} BMP4 and 10 ng ml^{-1} TGFβ3 at 3 d, but showed no differences in expression in response to 12.5 ng ml^{-1} BMP4 (figure 3(a)). *SOX9* and *SCX* expression were slightly increased following dosage with 200 ng ml^{-1} BMP4 (figures 3(b) and (c)). Groups treated with 200 ng ml^{-1} BMP4 had

significantly up-regulated expression of *SPP1* at 3 d, while groups treated with 12.5 ng ml^{-1} BMP4 had increased expression at 14 d (not significant) (figure 3(d)). Expression of *ACAN* was slightly increased following treatment with 12.5 ng ml^{-1} BMP4 at 14 d (figure 3(e)).

Immunofluoresence staining for collagen I, collagen II, aggrecan, decorin, osteopontin, and tenomodulin was also performed on 3D constructs to assess gene expression following exposure to the tested growth factors. Mixed expression of collagens I and II was observed in the no growth factor control and 12.5 ng ml^{-1} BMP4 group (figure 3(f)). Decreased expression of both collagens, but relative prevalence of collagen II, was seen following exposure to 200 ng ml^{-1} BMP4 and 10 ng ml^{-1} TGFβ3. Cells positive for aggrecan and decorin were seen across all samples (figure 3(g)). Groups treated with 12.5 ng ml^{-1} BMP4 and 10 ng ml^{-1} TGFβ3 had most cells stained weakly for decorin, with a few cells stained strongly for aggrecan. Notably, cells treated with 200 ng ml^{-1} BMP4 had the most cells stained strongly for aggrecan, with only a few stained for decorin. These trends are more notable than the no growth factor control, which showed mixed weak expression. The no growth factor control did not stain positive for osteopontin or tenomodulin (figure 3(h)). The group treated with 12.5 ng ml^{-1} BMP4 had slightly increased and mixed expression of osteopontin and tenomodulin. 200 ng ml^{-1} BMP4 was associated with highly increased expression of osteopontin and tenomodulin, with a mixed expression of both. The TGFβ3-treated group had most cells weakly positive for tenomodulin, with only a few visible cells positive for osteopontin.

3.3. MSCs exhibit heterogeneous response to 3D growth factor gradient

To assess the effect of spatial differences in growth factors, gels were cast with spatial loading of BMP4 and TGFβ3 as shown in figure 4(a). As shown, the top region of the gel was cast with 12.5 ng ml^{-1} of BMP4, the middle was cast with an increasing concentration of BMP4 from 12.5 ng ml^{-1} to 200 ng ml^{-1}, and the bottom was cast with 10 ng ml^{-1} TGFβ3.

Gene expression in cells isolated from the top, middle, and bottom regions of the gel was quantified using qPCR. An overall decrease in expression of *RUNX2, SOX9*, and *SCX* was seen in all regions of the multi-phasic group as compared to the no growth factor control (figures 4(b)–(f)). Interestingly, *SPP1* was up-regulated 2.3-fold in the top region, 4.8-fold in the middle, and 6-fold in the bottom region ($p = 0.02$), thus demonstrating spatial differences in expression (figure 4(e)). There was a trend of decreased expression of *ACAN*, as some regions did not detectably express this gene at the mRNA level (figure 4(f)).

Whole-gel constructs were stained using immunofluorescence and images were taken in each region (top, middle, and bottom) to assess protein expression and deposition. Images were quantified for the relative number of positively stained cells. Throughout the construct, cells expressed more collagen I and II than the no growth factor control (figures 4(h) and (k)). Relative levels of each type of collagen were similar throughout the construct, although the proportion of collagen II-positive cells was slightly higher in the middle region. Interestingly, the collagen staining shows apparent differences in cell morphology between the three regions; cells in the top of the gel were small and rounded, cells in the middle were large and rounded, and cells at the bottom were more spread and elongated, indicating

differences in cell spreading within the gel. We also stained for the tissue markers aggrecan, decorin, tenomodulin, and osteopontin. In the top region of the construct, cells predominantly expressed aggrecan while expressing very little decorin (figure 4(g)). However, in the middle region, cells expressed a mixture of both aggrecan and decorin, although typically not both. In the bottom region, cells were weakly positive for both aggrecan and decorin. Cells in the top and middle regions expressed more tenomodulin than at the bottom region, while the middle and bottom had slightly more osteopontin-positive cells than the top region (figure 4(i)). This corresponds with the PCR finding in figure 4(e) of increased *SPP1* expression, which was highest in the bottom region of the construct. Quantification of the proportion of positive cells within each region, shown in figures 4(j)–(k), reiterate the trends observed in the images. Overall, there are differences in protein deposition within the multi-phasic gel.

4. Discussion

The human body is unable to regenerate the bone-tendon enthesis following injury or surgical repair, and thus tissue engineering provides a potential strategy to replace this tissue. Strategies for engineering multiphasic musculoskeletal tissues can be applied to the bone-tendon enthesis and vice versa. Cellularized approaches are limited by low availability of primary cells; therefore, the incorporation of stem cells presents a more practical solution. Previous studies utilizing spatial growth factor presentation to induce spatial phenotypic differences in MSCs were limited by their simplistic growth factor lay-outs, such as only including two distinct regions, or a gradient of a single growth factor [33, 35]. Therefore, the objective of this study was to develop a hydrogel construct with spatially patterned growth factors to induce differing phenotypic responses throughout the gel. It was hypothesized that following fabrication of a patterned construct, MSC phenotype would vary throughout the multi-phasic construct.

MSC differentiation is a complex process requiring a multitude of biochemical factors, resulting in complex changes in gene and protein expression. The response to the growth factors used in this study was not always straightforward, which exemplifies the complexity of differentiation pathways [20, 36, 37]. Based on previous studies, it was expected that BMP4 would induce osteogenic differentiation [15, 38], TGFβ3 would induce chondrogenic or tenogenic differentiation [39, 40], and BMP12 would induce tenogenic differentiation with largely dose-independent effects [35, 41]. Furthermore, we were interested in understanding how differentiation in response to growth factors in 2D related to differentiation in 3D.

Overall, 3D protein deposition was consistent with protein deposition and gene expression from the 2D culture studies, with the emergence of expression of other proteins due to the heterogeneous behavior observed in 3D. In the single growth factor 2D studies, 12.5 ng ml^{-1} BMP4 resulted in changes consistent with osteogenesis, including increased *RUNX2,* osteopontin, and decorin expression. Despite evidence that MSC differentiation in response to growth factors differs in a 3D versus 2D environment [42, 43], similar trends in osteogenic gene and protein expression were observed in the single-growth factor 3D studies. Furthermore, a higher concentration of BMP4 (200 ng ml^{-1}) resulted in significantly

increased *ACAN* gene expression in 2D, an effect which was further increased at the protein level in 3D. The increased expression of chondrogenic markers compared to the control and other treatment groups suggests that 200 ng ml^{-1} of BMP4 in a 2D and 3D environment induces chondrogenic differentiation. Other studies have also found up-regulation of *RUNX2* and *SPP1* in response to concentrations of BMP4 from 20–800 ng ml^{-1} [15, 38, 44, 45], and some have found up-regulation of *ACAN* in response to BMP4 from 10–100 ng ml^{-1} [46, 47], indicating that BMP4 may have roles in both osteogenic and chondrogenic differentiation, which is supported by the results from our study. Thus, these results supported utilizing a gradient of BMP4 in the osteogenic to chondrogenic phases of the multiphasic scaffold.

TGFβ3 was hypothesized to induce differentiation towards chondrogenic and tenogenic lineages. In 2D culture, TGFβ3 treatment resulted in up-regulation of each gene assayed except *ACAN*, implicating non-specific increases in musculoskeletal lineage marker expression [48], which is supported by other studies which have documented increased expression of *RUNX2, SOX9, ACAN, SCX*, and *TNMD* in response to TGFβ3 at concentrations from 5–20 ng ml^{-1} [49, 54]. In 2D, gene expression changes only translated to the protein expression of chondrogenic markers, including increased expression of collagen II and aggrecan, compared to the control and all other treatment groups. In 3D culture, protein expression was more indicative of heterogeneous differentiation towards tenogenic or chondrogenic lineages, as evidenced by staining for decorin, aggrecan, and tenomodulin proteoglycans. The heterogeneous response of cells to TGFβ3 in both 2D and 3D has been established by Cote *et al*, who found single-cell heterogeneity in gene expression changes, most remarkably in aggrecan, which did not necessarily correlate with protein deposition at the single-cell or whole population level [55], which helps explain why we did not observe changes in *ACAN* mRNA in response to TGFβ3 at the gene expression level. Furthermore, the authors observed that some cells expressed aggrecan as well as osteopontin, indicating some lineage-inappropriate gene expression profiles [55]. Other studies have implicated TGFβ3 in chondrogenesis and tenogenesis during endochondral ossification, as well as *in vitro* differentiation of MSCs [21, 54, 56, 57], suggesting that TGFβ3 is involved in multiple differentiation pathways, supporting the idea that some of these cells have differentiated towards a multipotent precursor of chondrocytes and tenocytes [36, 58]. Overall, the consistent expression of chondrogenic and tenogenic markers indicate heterogeneous commitment to fibrochondrocyte- and tenocyte-like populations [21, 54, 56].

BMP12, contrary to the hypothesis, did not result in any distinct changes in gene expression regardless of concentration used, which has been seen else-where [59, 60]. There is conflicting evidence regarding the ability of BMP12 to induce changes in expression of tenogenic genes in MSCs, with some finding increased expression [61, 63], and others finding no changes [59, 60]. Studies looking at osteogenic markers and chondrogenic markers are largely consistent with ours, which showed no changes in *RUNX2* expression, with the exception of one study finding increased *ACAN* expression [61, 64]. These results may be reflective of BMP12's involvement in later stages of tenogenic differentiation and matrix production [60, 65], and thus may not be able to induce differentiation on its own. Therefore, we chose not to continue utilizing this growth factor in later studies, and thus differentiation in response to BMP12 was not assessed in 3D in single growth factor or

multiphasic constructs. Overall, our results reveal that 2D culture is a predictor of differentiation of MSCs in response to growth factors in GelMA. This supports the continued use of 2D-validated growth factors in 3D GelMA constructs.

Including a gradient of BMP4 and a region of TGFβ3 in the multi-phasic construct was logical based on the results in the single growth factor studies and evidence that these growth factors play a similar role in the development of the bone-tendon enthesis [66]. The casted construct was similar to the growth factor patterning present during development and was supported by the 2D and 3D results in this study; the construct contained a gradient of BMP4 from a low (12.5 ng ml^{-1}) to high (200 ng ml^{-1}) concentration, followed by a block of TGFβ3 in the remaining third (figure 4(a)). The spatial differences in osteopontin, aggrecan, tenomodulin, and collagen protein deposition, and *SPP1* gene expression, indicate that this system does result in spatial differences in MSC response as hypothesized. In the top region, expression of osteopontin and collagen I indicates a tendency towards osteogenesis. In the middle region, cells expressed a combination of chondrogenic, osteogenic, and tenogenic proteins indicating that cells were differentiating in a non-uniform manner and that the cell populations in this part of the construct were heterogenous [67, 68]. Finally, the decorin and aggrecan staining, presence of collagen I, and expression of osteopontin and tenomodulin may indicate differentiation down a tenogenic or fibrochondrogenic pathway distinct from that which is seen in the middle or top regions of the scaffold. The heterogeneous response was intriguing, albeit not surprising, as the starting population of MSCs was likely heterogeneous, as has been extensively described [69, 72].

There have been a multitude of approaches to fabricating multi-phasic constructs for multi-lineage differentiation, although many similar examples are for the osteochondral or meniscus interface, not the bone-tendon enthesis. For example, a study by Li *et al* developed a construct with covalently bound BMP2 and TGFβ3 in opposing gradients in a PLGA scaffold. It was observed that MSCs had spatial differences in collagen X and osteopontin expression in response to this layout, indicating that this system presented appropriate growth factor concentrations for an adequate period of time to induce spatial differences [34]. One drawback of the results of this study was that there were no spatial differences in the key structural proteins collagen I and II, indicating that while this layout was sufficient to induce differentiation, it was not sufficient to recapitulate key structural components. Spatial differences in growth factor presentation developed using inkjet printing of hydrogels have also demonstrated the ability to develop distinct phases resulting in distinct cell phenotypes, including differences in morphology and protein secretion [73, 74]. A study by Gurkan *et al* used micropatterning of distinct droplets of growth factors to observe increased expression of osteogenic and chondrogenic genes, although the small nature of the printed constructs meant that expression could not be regionally determined [73]. Although these studies were beneficial in demonstrating proof of concept for utilizing growth factors to induce spatial differentiation, inkjet printing is not practical for large constructs. Furthermore, it is more difficult to create a true gradient with inkjet printing. A study by Font Tellado *et al*, one of the few studies intended for the application of the bone-tendon enthesis, used heparin-bound TGFβ2 and BMP14 in two distinct phases. This approach resulted in no regional differences in gene expression or protein expression, which may have been due to its inability to spatially retain growth factors or due to issues with the growth factors used [35].

Specifically, evidence for the use of TGFβ2 and BMP14 for inducing terminal differentiation into any musculoskeletal lineage *in vitro* remains minimal [20]. The common denominator in these studies is that both the temporal and spatial presentation were ultimately associated with spatial differences in cellular behaviour, as was observed in this study.

In the context of these results, it is important to consider how the bioactivity of growth factors within GelMA may have influenced the results observed. It is well characterized that growth factors have short half-lives, in the order of hours, and are degraded quickly both *in vivo* and *in vitro* [75, 76]. Therefore, both the bioactivity and concentration decreased over time. In this study, the highest concentration of bioactive growth factor was present in the initial hydrogel precursor solution with the bioactive concentration decreasing slowly over time. Therefore, it is probable that the heterogeneous effects observed are largely a result of initial signaling within the precursor solution, as well as the remaining bioactive growth factor within the first day. As previously mentioned, it has also been shown that gelatin and GelMA can electrostatically bind growth factors such as fibroblast growth factor (FGF) [25, 77]. The electrostatic binding, and sustained release, from these hydrogels can improve retention of bioactivity following release *in vivo*, thus sustaining the presence of bioactive growth factors for longer than a dose of free growth factors [23, 78]. While these delivery vehicles did not include cells, it is possible that the use of GelMA as the hydrogel in this study prolonged the bioactivity of the growth factors. Regardless, it is likely that the results observed are from both the initial signaling during fabrication, and a sustained low dose of bioactive growth factor within the construct, resulting in concurrent differentiation of MSCs. That being said, it is also important to note that MSC response to different microenvironments can vary from donor to donor and source to source [69, 79], and thus future studies should assess whether the trends observed in this paper hold true for different populations of cells.

Furthermore, another limitation is the lack of mechanical characterization in fabrication of an orthopaedic tissue. As previously stated, our objective was to study spatially patterned growth factors to induce differing phenotypic responses throughout the hydrogel, and thus focused on the biochemical characterization and cells' phenotypic response of this construct. We acknowledge that mechanical stimuli influences cell differentiation and response to growth factors [42, 80, 81], and this was not considered herein, though it is of interest in future studies. Additionally, we did not assess UV penetration as a fundamental parameter of the system, where poor penetration could lead to reduced crosslinking between layers, with potential slipping. Instead, we assumed that retention of the gross bulk shape of the construct (i.e. a full cylindrical shape over 14 d) was sufficient. However, detailed mechanical characterization could prove useful for future studies, particularly as future studies seek to utilize additional biochemical components, such as multiple, sequentially dosed growth factors, hydroxyapatite, or ECM components within hydrogel-based approaches for engineering mechanically rigorous orthopaedic tissue [22, 82, 86].

5. Conclusions

This study develops and validates a novel multiphasic GelMA construct for spatial presentation of growth factors with single-concentration and gradient regions for inducing a spatially varying MSC phenotype. It was determined, through development of a construct with fluorescently tagged proteins, that sequential layering of GelMA could be used to pattern protein within a construct. TGFβ family growth factors loaded into the construct affect the expression of osteogenic, chondrogenic, and tenogenic lineage protein and gene markers, with spatial loading resulting in a spatially heterogeneous response. While this study utilizes this system for the bone-tendon enthesis, it is applicable on a broader scale for engineering other musculoskeletal interfaces and complex tissues, and demonstrates increased complexity of spatial presentation of biochemical factors, thus remaining a promising approach for engineering the bone-tendon enthesis.

Acknowledgments

This work was funded by the National Institutes of Health/National Institute of Biomedical Imaging and Bioengineering Center for Engineering Complex Tissues (P41 EB023833).

References

[1]. Clayton RAE and Court-Brown CM 2008 The epidemiology of musculoskeletal tendinous and ligamentous injuries Injury 39 1338–44 [PubMed: 19036362]

[2]. Dodson CC, Kitay A, Verma NN, Adler RS, Nguyen J, Cordasco FA and Altchek DW 2010 The long-term outcome of recurrent defects after rotator cuff repair Am. J. Sports Med 38 35–9 [PubMed: 19752204]

[3]. Elia F et al. 2017 Clinical and anatomic results of surgical repair of chronic rotator cuff tears at ten-year minimum follow-up Int. Orthop 41 1219–26 [PubMed: 28382384]

[4]. Jost B, Zumstein M, Pfirrmann CWA and Gerber C 2006 Long-term outcome after structural failure of rotator cuff repairs J. Bone Jt. Surg Am 88 472–9

[5]. Sano H, Yamashita T, Wakabayashi I and Itoi E 2007 Stress distribution in the supraspinatus tendon after tendon repair: suture anchors versus transosseous suture fixation Am. J. Sports Med 35 542–6 [PubMed: 17218657]

[6]. Tan H, Wang D, Lebaschi AH, Hutchinson ID, Ying L, Deng X-H, Rodeo SA and Warren RF 2018 Comparison of bone tunnel and cortical surface tendon-to-bone healing in a rabbit model of biceps tenodesis J. Bone Jt. Surg. Am 100 479–86

[7]. Killian ML, Cavinatto L, Galatz LM and Thomopoulos S 2012 Recent advances in shoulder research Arthritis Res. Ther 14 214 [PubMed: 22709417]

[8]. Moffat KL, Sun W-HS, Pena PE, Chahine NO, Doty SB, Ateshian GA, Hung CT and Lu HH 2008 Characterization of the structure–function relationship at the ligament-to-bone interface Proc. Natl. Acad. Sci 105 7947–52 [PubMed: 18541916]

[9]. Benjamin M, Toumi H, Ralphs JR, Bydder G, Best TM and Milz S 2006 Where tendons and ligaments meet bone: attachment sites (‘entheses’) in relation to exercise and/or mechanical load J. Anat 208 471–90 [PubMed: 16637873]

[10]. Cheung EV, Silverio L and Sperling JW 2010 Strategies in biologic augmentation of rotator cuff repair: a review Clin. Orthop 468 1476–84 [PubMed: 20352390]

[11]. Benjamin M et al. 2002 The skeletal attachment of tendons—tendon ‘entheses’ Comp. Biochem. Physiol. A Mol. Integr. Physiol 133 931–45 [PubMed: 12485684]

[12]. Lam J, Lu S, Meretoja VV, Tabata Y, Mikos AG and Kasper FK 2014 Generation of osteochondral tissue constructs with chondrogenically and osteogenically predifferentiated mesenchymal stem cells encapsulated in bilayered hydrogels Acta Biomater. 10 1112–23 [PubMed: 24300948]

[13]. Huynh NPT et al. 2018 Genetic engineering of mesenchymal stem cells for differential matrix deposition on 3D woven scaffolds Tissue Eng. Part A 24 1531–44 [PubMed: 29756533]

[14]. Chen X et al. 2013 Chondrogenic differentiation of umbilical cord-derived mesenchymal stem cells in type I collagen-hydrogel for cartilage engineering Injury 44 540–9 [PubMed: 23337703]

[15]. Friedman MS, Long MW and Hankenson KD 2006 Osteogenic differentiation of human mesenchymal stem cells is regulated by bone morphogenetic protein-6 J. Cell. Biochem 98 538–54 [PubMed: 16317727]

[16]. Igura K, Zhang X, Takahashi K, Mitsuru A, Yamaguchi S and Takahashi TA 2004 Isolation and characterization of mesenchymal progenitor cells from chorionic villi of human placenta Cytotherapy 6 543–53 [PubMed: 15770794]

[17]. Rossello RA and Kohn DH 2010 Cell communication and tissue engineering Commun. Integr. Biol 3 53–6 [PubMed: 20539784]

[18]. Font Tellado S, Balmayor ER and Van Griensven M 2015 Strategies to engineer tendon/ligament-to-bone interface: biomaterials, cells and growth factors Adv. Drug Deliv. Rev 94 126–40 [PubMed: 25777059]

[19]. Graycar JL, Miller DA, Arrick BA, Lyons RM, Moses HL and Derynck R 1989 Human transforming growth factor-β3: recombinant expression, purification, and biological activities in comparison with transforming growth factors-β 1 and -β2 Mol. Endocrinol 3 1977–86 [PubMed: 2628733]

[20]. Grafe I. et al. 2017; TGF-b family signaling in mesenchymal differentiation. Cold Spring Harb. Prospect. Biol. 10:a022202.

[21]. Matsunaga S, Yamamoto T and Fukumura K 1999 Temporal and spatial expressions of transforming growth factor-betas and their receptors in epiphyseal growth plate Int. J. Oncol 14 1063–70 [PubMed: 10339658]

[22]. Brown GCJ, Lim KS, Farrugia BL, Hooper GJ and Woodfield TBF 2017 Covalent incorporation of heparin improves chondrogenesis in photocurable gelatin-methacryloyl hydrogels Macromol. Biosci 17 1700158

[23]. Teotia AK, Gupta A, Raina DB, Lidgren L and Kumar A 2016 Gelatin-modified bone substitute with bioactive molecules enhance cellular interactions and bone regeneration Appl. Mater. Interfaces 8 10775–87

[24]. Klotz BJ, Gawlitta D, Rosenberg AJWP, Malda J and Melchels FPW 2016 Gelatin-methacryloyl hydrogels: towards biofabrication-based tissue repair Trends Biotechnol. 34 394–407 [PubMed: 26867787]

[25]. Nguyen AH, McKinney J, Miller T, Bongiorno T and McDevitt TC 2015 Gelatin methacrylate microspheres for controlled growth factor release Acta Biomater. 13 101–10 [PubMed: 25463489]

[26]. Piard C, Baker H, Kamalitdinov T and Fisher JP 2019 Bioprinted osteon-like scaffolds enhance *in vivo* neovascularization Biofabrication 11 025013 [PubMed: 30769337]

[27]. Piard C, Jeyaram A, Liu Y, Caccamese J, Jay SM, Chen Y and Fisher J 2019 3D printed HUVECs/MSCs cocultures impact cellular interactions and angiogenesis depending on cell–cell distance Biomaterials 222 119423 [PubMed: 31442885]

[28]. Kuo C-Y, Eranki A, Placone JK, Rhodes KR, Aranda-Espinoza H, Fernandes R, Fisher JP and Kim PCW 2016 Development of a 3D printed, bioengineered placenta model to evaluate the role of trophoblast migration in preeclampsia ACS Biomater. Sci. Eng 2 1817–26

[29]. Wu Y, Puperi DS, Grande-Allen KJ and West JL 2017 Ascorbic acid promotes extracellular matrix deposition while preserving valve interstitial cell quiescence within 3D hydrogel scaffolds J. Tissue Eng. Regen. Med 11 1963–73 [PubMed: 26631842]

[30]. Schindelin J et al. 2012 Fiji: an open-source platform for biological-image analysis Nat. Methods 9 676–82 [PubMed: 22743772]

[31]. Haimov-Kochman R, Fisher SJ and Winn VD 2006 Modification of the standard trizol-based technique improves the integrity of RNA isolated from RNase-rich placental tissue Clin. Chem 52 159–60 [PubMed: 16391340]

[32]. Livak KJ and Schmittgen TD 2001 Analysis of relative gene expression data using real-time quantitative PCR and the $2^{(-\Delta\Delta CT)}$ method Methods 25 402–8 [PubMed: 11846609]

[33]. Di Luca A. et al. 2017; Covalent binding of bone morphogenetic protein 2 and transforming growth factor-β3 to 3D plotted scaffolds for osteochondral tissue engineering. Biotechnol. J. 12:1700072.

[34]. Li C et al. 2018 Glycosylated and superparamagnetic nanoparticle gradients for osteochondral tissue engineering Biomaterials 176 24–33 [PubMed: 29852377]

[35]. Font Tellado S, Chiera S, Bonani W, Poh PSP, Migliaresi C, Motta A, Balmayor ER and van Griensven M 2018 Heparin functionalization increases retention of TGF-β2 and GDF5 on biphasic silk fibroin scaffolds for tendon/ligament-to-bone tissue engineering Acta Biomater. 72 150–66 [PubMed: 29550439]

[36]. Asou Y, Nifuji A, Tsuji K, Shinomiya K, Olson EN, Koopman P and Noda M 2002 Coordinated expression of scleraxis and Sox9 genes during embryonic development of tendons and cartilage J. Orthop. Res 20 827–33 [PubMed: 12168674]

[37]. Cleary MA, van Osch GJVM, Brama PA, Hellingman CA and Narcisi R 2015 FGF, TGFβ and Wnt crosstalk: embryonic to *in vitro* cartilage development from mesenchymal stem cells J. Tissue Eng. Regen. Med 9 332–42 [PubMed: 23576364]

[38]. Sammons J, Ahmed N, El-Sheemy M and Hassan HT 2004 The role of BMP-6, IL-6, and BMP-4 in mesenchymal stem cell-dependent bone development: effects on osteoblastic differentiation induced by parathyroid hormone and vitamin D3 Stem Cells Dev. 13 273–80 [PubMed: 15186723]

[39]. Pittenger MF et al. 1999 Multilineage potential of adult human mesenchymal stem cells Science 284 143–7 [PubMed: 10102814]

[40]. Yang G, Rothrauff BB, Lin H, Gottardi R, Alexander PG and Tuan RS 2013 Enhancement of tenogenic differentiation of human adipose stem cells by tendon-derived extracellular matrix Biomaterials 34 9295–306 [PubMed: 24044998]

[41]. Lee JY. et al. 2011; BMP-12 treatment of adult mesenchymal stem cells *in vitro* augments tendon-like tissue formation and defect repair *in vivo*. PLoS ONE. 6:e17531. [PubMed: 21412429]

[42]. Baker BM and Chen CS 2012 Deconstructing the third dimension – how 3D culture microenvironments alter cellular cues J. Cell. Sci 125 3015–24 [PubMed: 22797912]

[43]. Caliari SR, Vega SL, Kwon M, Soulas EM and Burdick JA 2016 Dimensionality and spreading influence MSC YAP/TAZ signaling in hydrogel environments Biomaterials 103 314–23 [PubMed: 27429252]

[44]. Maeda S, Hayashi M, Komiya S, Imamura T and Miyazono K 2004 Endogenous TGF-β signaling suppresses maturation of osteoblastic mesenchymal cells EMBO J. 23 552–63 [PubMed: 14749725]

[45]. Hu Z-M, Peel SAF, Ho SKC, Sandor GKB and Clokie CML 2009 Comparison of platelet-rich plasma, bovine BMP, and rhBMP-4 on bone matrix protein expression *in vitro* Growth Factors 27 280–8 [PubMed: 19637071]

[46]. Azumi E, Honda Y, Kishimoto N, Hashimoto Y and Matsumoto N 2016 Gene expression profiles of early chondrogenic markers in dedifferentiated fat cells stimulated by bone morphogenetic protein 4 under monolayer and spheroid culture conditions *in vitro* Orthod. Waves 75 97–104

[47]. Steinert A, Weber M, Dimmler A, Julius C, Schütze N, Nöth U, Cramer H, Eulert J, Zimmermann U and Hendrich C 2003 Chondrogenic differentiation of mesenchymal progenitor cells encapsulated in ultrahigh-viscosity alginate J. Orthop. Res 21 1090–7 [PubMed: 14554223]

[48]. Gregory CA, Ylostalo J and Prockop DJ 2005 Adult bone marrow stem/progenitor cells (MSCs) are preconditioned by microenvironmental ‘niches’ in culture: a two-stage hypothesis for regulation of MSC fate Sci. Signal 2005 pe37

[49]. Rich JT, Rosová I, Nolta JA, Myckatyn TM, Sandell LJ and McAlinden A 2008 Upregulation of *Runx2* and *Osterix* during *in vitro* chondrogenesis of human adipose-derived stromal cells Biochem. Biophys. Res. Commun 372 230–5 [PubMed: 18482578]

[50]. Arita NA, Pelaez D and Cheung HS 2011 Activation of the extracellular signal-regulated kinases 1 and 2 (ERK1/2) is needed for the TGFβ-induced chondrogenic and osteogenic differentiation of mesenchymal stem cells Biochem. Biophys. Res. Commun 405 564–9 [PubMed: 21262199]

[51]. Hara ES, Ono M, Yoshioka Y, Ueda J, Hazehara Y, Pham HT, Matsumoto T and Kuboki T 2016 Antagonistic effects of insulin and TGF-β3 during chondrogenic differentiation of human BMSCs under a minimal amount of factors Cells Tissues Organs 201 88–96 [PubMed: 26866713]

[52]. Bhang SH, Jeon J-Y, La W-G, Seong JY, Hwang JW, Ryu SE and Kim B-S 2011 Enhanced chondrogenic marker expression of human mesenchymal stem cells by interaction with both TGF-β3 and hyaluronic acid Biotechnol. Appl. Biochem 58 271–6 [PubMed: 21838802]

[53]. Yu Y, Lee SY, Yang E-J, Kim HY, Jo I and Shin S-J 2016 Expression of tenocyte lineage-related factors from tonsil-derived mesenchymal stem cells Tissue Eng. Regen. Med 13 162–70 [PubMed: 30603396]

[54]. Yang G, Rothrauff BB, Lin H, Yu S and Tuan RS 2016 Tendon-derived extracellular matrix enhances transforming growth factor-β3-induced tenogenic differentiation of human adipose-derived stem cells Tissue Eng. Part A 23 166–76

[55]. Cote AJ, McLeod CM, Farrell MJ, McClanahan PD, Dunagin MC, Raj A and Mauck RL 2016 Single-cell differences in matrix gene expression do not predict matrix deposition Nat. Commun 7 1–13

[56]. Weiss S, Hennig T, Bock R, Steck E and Richter W 2010 Impact of growth factors and PTHrP on early and late chondrogenic differentiation of human mesenchymal stem cells J. Cell. Physiol 223 84–93 [PubMed: 20049852]

[57]. Liu D-D, Zhang J-C, Zhang Q, Wang S-X and Yang M-S 2013 TGF-β/BMP signaling pathway is involved in cerium-promoted osteogenic differentiation of mesenchymal stem cells J. Cell. Biochem 114 1105–14 [PubMed: 23150386]

[58]. Ferguson GB. et al. 2018; Mapping molecular landmarks of human skeletal ontogeny and pluripotent stem cell-derived articular chondrocytes. Nat. Commun. 9:3634. [PubMed: 30194383]

[59]. Kishore V, Bullock W, Sun X, Van Dyke WS and Akkus O 2012 Tenogenic differentiation of human MSCs induced by the topography of electrochemically aligned collagen threads Biomaterials 33 2137–44 [PubMed: 22177622]

[60]. Yin Z et al. 2016 Stepwise differentiation of mesenchymal stem cells augments tendon-like tissue formation and defect repair *in vivo* Stem Cell Trans. Med 5 1106–16

[61]. Shen H, Gelberman RH, Silva MJ, Sakiyama-Elbert SE and Thomopoulos S 2013 BMP12 induces tenogenic differentiation of adipose-derived stromal cells PLoS ONE 8 e77613 [PubMed: 24155967]

[62]. Rajpar I and Barrett JG 2019 Optimizing growth factor induction of tenogenesis in three-dimensional culture of mesenchymal stem cells J. Tissue Eng 10 2041731419848776 [PubMed: 31205672]

[63]. Otabe K et al. 2015 Transcription factor Mohawk controls tenogenic differentiation of bone marrow mesenchymal stem cells *in vitro* and *in vivo* J. Orthop. Res 33 1–8 [PubMed: 25312837]

[64]. Yeh L-C-C and Lee JC 2010 Effects of cartilage-derived morphogenetic protein-3 on the expression of chondrogenic and osteoblastic markers in the pluripotent mesenchymal C3H10T1/2 cell line Growth Factors 28 117–28 [PubMed: 20102312]

[65]. Fu SC, Wong YP, Chan BP, Pau HM, Cheuk YC, Lee KM and Chan K-M 2003 The roles of bone morphogenetic protein (BMP) 12 in stimulating the proliferation and matrix production of human patellar tendon fibroblasts Life Sci. 72 2965–74 [PubMed: 12706484]

[66]. Zelzer E, Blitz E, Killian ML and Thomopoulos S 2014 Tendon-to-bone attachment: from development to maturity Birth Defects Res. Part C Embryo Today Rev 102 101–12

[67]. Shafiee A, Seyedjafari E, Soleimani M, Ahmadbeigi N, Dinarvand P and Ghaemi N 2011 A comparison between osteogenic differentiation of human unrestricted somatic stem cells and mesenchymal stem cells from bone marrow and adipose tissue Biotechnol. Lett 33 1257–64 [PubMed: 21287233]

[68]. Rowland CR, Lennon DP, Caplan AI and Guilak F 2013 The effects of crosslinking of scaffolds engineered from cartilage ECM on the chondrogenic differentiation of MSCs Biomaterials 34 5802–12 [PubMed: 23642532]

[69]. Anker PIT et al. 2003 Mesenchymal stem cells in human second-trimester bone marrow, liver, lung, and spleen exhibit a similar immunophenotype but a heterogeneous multilineage differentiation potential Haematologica 88 845–52 [PubMed: 12935972]

[70]. Phinney DG 2012 Functional heterogeneity of mesenchymal stem cells: implications for cell therapy J. Cell. Biochem 113 2806–12 [PubMed: 22511358]

[71]. Pevsner-Fischer M, Levin S and Zipori D 2011 The origins of mesenchymal stromal cell heterogeneity Stem Cell Rev. Rep 7 560–8 [PubMed: 21437576]

[72]. Ho PA, Wagner W and Franke W 2008 Heterogeneity of mesenchymal stromal cell preparations Cytotherapy 10 320–30 [PubMed: 18574765]

[73]. Gurkan UA, El Assal R, Yildiz SE, Sung Y, Trachtenberg AJ, Kuo WP and Demirci U 2014 Engineering anisotropic biomimetic fibrocartilage microenvironment by bioprinting mesenchymal stem cells in nanoliter gel droplets Mol. Pharm 11 2151–9 [PubMed: 24495169]

[74]. Ker EDF, Chu B, Phillippi JA, Gharaibeh B, Huard J, Weiss LE and Campbell PG 2011 Engineering spatial control of multiple differentiation fates within a stem cell population Biomaterials 32 3413–22 [PubMed: 21316755]

[75]. Suliman S et al. 2015 Release and bioactivity of bone morphogenetic protein-2 are affected by scaffold binding techniques *in vitro* and *in vivo* J. Control. Release 197 148–57 [PubMed: 25445698]

[76]. Zhao B, Katagiri T, Toyoda H, Takada T, Yanai T, Fukuda T, Chung U-I, Koike T, Takaoka K and Kamijo R 2006 Heparin potentiates the *in vivo* ectopic bone formation induced by bone morphogenetic protein-2 J. Biol. Chem 281 23246–53 [PubMed: 16754660]

[77]. Young S, Wong M, Tabata Y and Mikos AG 2005 Gelatin as a delivery vehicle for the controlled release of bioactive molecules J. Control. Release 109 256–74 [PubMed: 16266768]

[78]. Kimura Y, Ozeki M, Inamoto T and Tabata Y 2003 Adipose tissue engineering based on human preadipocytes combined with gelatin microspheres containing basic fibroblast growth factor Biomaterials 24 2513–21 [PubMed: 12695078]

[79]. Siegel G, Kluba T, Hermanutz-Klein U, Bieback K, Northoff H and Schäfer R 2013 Phenotype, donor age and gender affect function of human bone marrow-derived mesenchymal stromal cells BMC Med. 11 1–20 [PubMed: 23281898]

[80]. Engler AJ, Sen S, Sweeney HL and Discher DE 2006 Matrix elasticity directs stem cell lineage specification Cell 126 677–89 [PubMed: 16923388]

[81]. Pek YS, Wan ACA and Ying JY 2010 The effect of matrix stiffness on mesenchymal stem cell differentiation in a 3D thixotropic gel Biomaterials 31 385–91 [PubMed: 19811817]

[82]. Gegg C and Yang F 2020 Spatially patterned microribbon-based hydrogels induce zonally-organized cartilage regeneration by stem cells in 3D Acta Biomater. 101 196–205 [PubMed: 31634627]

[83]. Bartnikowski M, Akkineni AR, Gelinsky M, Woodruff MA and Klein TJ 2016 Hydrogel model incorporating 3D-plotted hydroxyapatite for osteochondral tissue engineering Materials 9 285

[84]. Idaszek J. et al. 2019; 3D bioprinting of hydrogel constructs with cell and material gradients for the regeneration of full-thickness chondral defect using a microfluidic printing head. Biofabrication. 11:044101. [PubMed: 31151123]

[85]. Dormer NH, Singh M, Wang L, Berkland CJ and Detamore MS 2010 Osteochondral interface tissue engineering using macroscopic gradients of bioactive signals Ann. Biomed. Eng 38 2167–82 [PubMed: 20379780]

[86]. Mellor LF et al. 2019 Investigation of multiphasic 3D-bioplotted scaffolds for site-specific chondrogenic and osteogenic differentiation of human adipose-derived stem cells for osteochondral tissue engineering applications J. Biomed. Mater. Res. B Appl. Biomater 108 2017–30 [PubMed: 31880408]

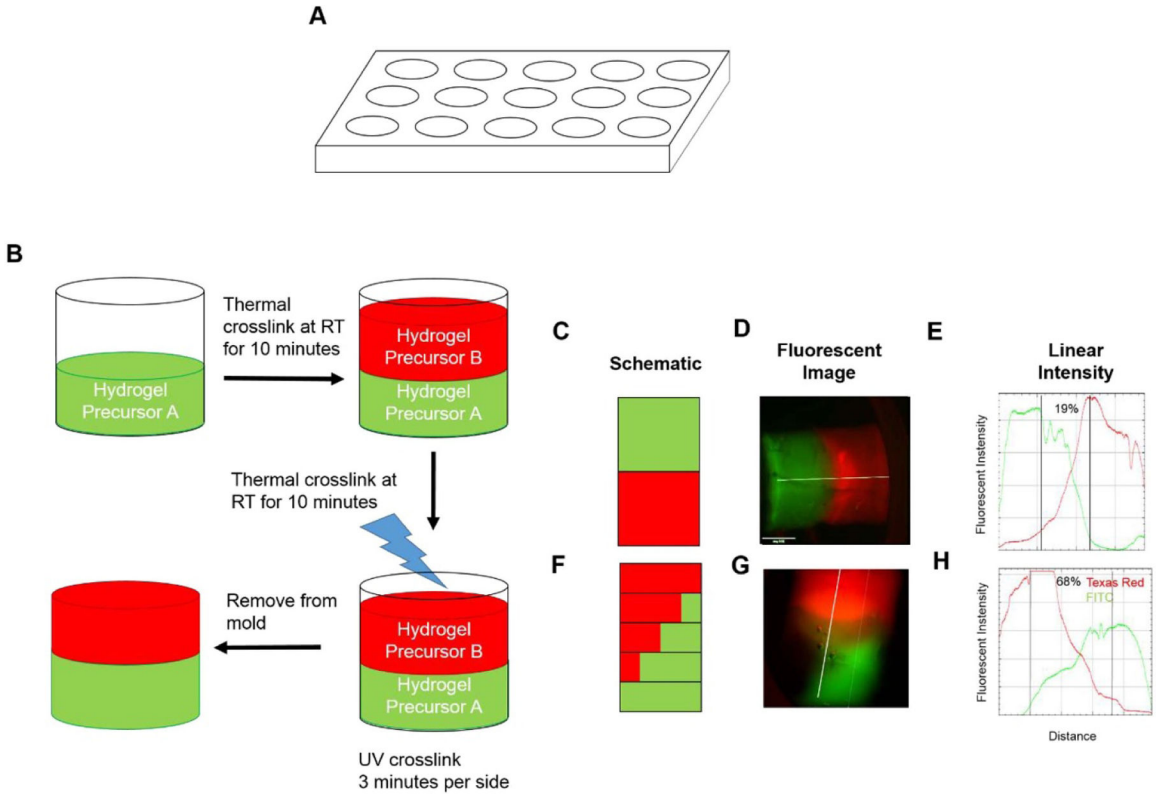

Figure 1.

Fabrication of multi-phasic hydrogels. (a) Schematic of mold used for fabrication. (b) Schematic of fabrication method of multi-phasic hydrogels. Hydrogel precursor solution is layered with thermal crosslinking between layers before final UV crosslinking. (c), (f) Schematic of spatial organization of multi-phasic scaffolds. Note that each outlined box is a layer within the scaffold. Detailed explanation of fabrication of constructs corresponding to schematics (c) and (f) can be found in table 1. (d), (g) Representative fluorescent images of multi-phasic hydrogels containing fluorescently tagged BSA immediately following crosslinking. (e), (h) Representative graphs of linear intensity of fluorescent images from hydrogels in panels (d) and (g), respectively. Data are presented as representative images. Scale bar = 1 mm.

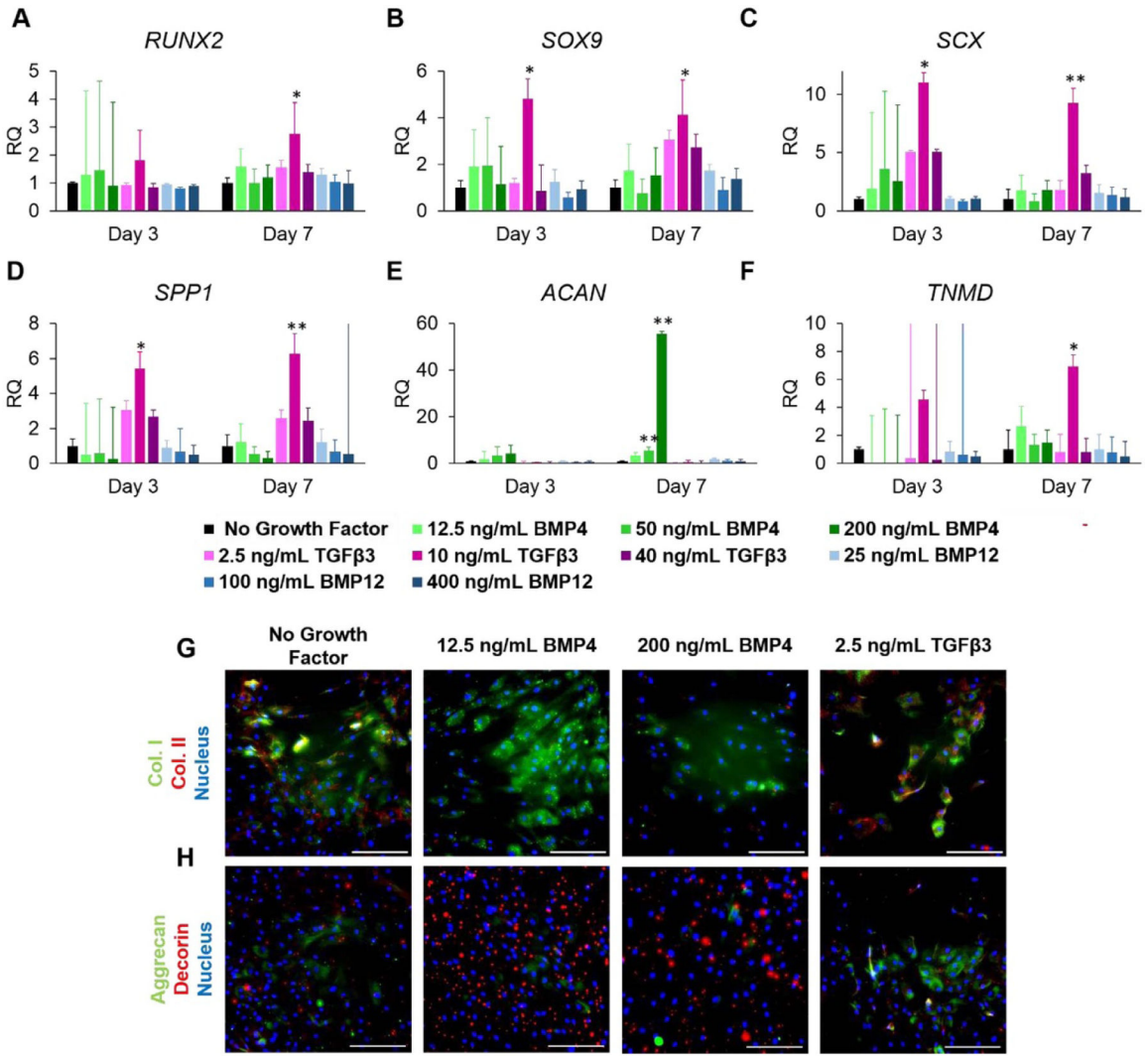

Figure 2.

Influence of growth factors BMP4, TGFβ3, and BMP12 dosage concentration on MSC gene and protein expression in 2D culture. (a)–(f) Relative expression of (a) *RUNX2*, (b) *SOX9*, (c) *SCX*, (d) *SPP1*, (e) *ACAN*, and (f) *TNMD*. (g), (h) Immunofluorescence staining of MSCs dosed at 12.5 ng ml^{-1} BMP4, 200 ng ml^{-1} BMP4, and 2.5 ng ml^{-1} TGFβ3 for (g) collagen I (green), collagen II (red), and nucleus (blue) and (h) aggrecan (green), decorin (red), and nucleus (blue). * indicates $p < 0.05$, ** indicates $p < 0.0001$ compared to the no growth factor control. Values are presented as mean ± SD. Scale bar = 100 μm.

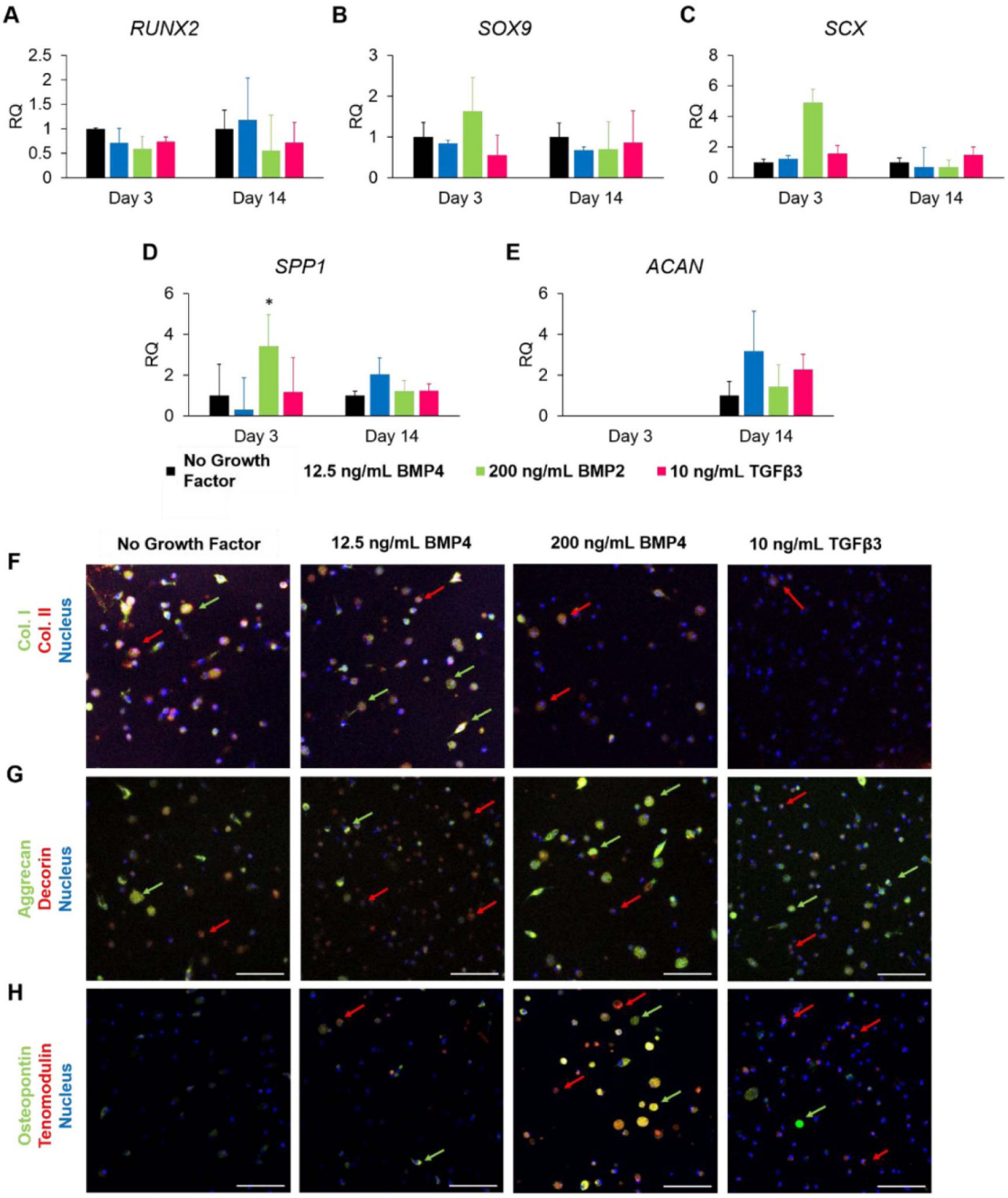

Figure 3.

MSC gene and protein expression in response to 12.5 ng ml^{-1} BMP4, 200 ng ml^{-1} BMP4, and 10 ng ml^{-1} TGFβ3 in 3D culture. (a)–(e) Relative expression of (a) *RUNX2*, (b) *SOX9*, (c) Scleraxis, (d) osteopontin, and (e) aggrecan. (f)–(i) Immunofluorescence staining for (f) collagen I (green) and collagen II (red), (g) aggrecan (green) and decorin (red), and (h) osteopontin (green) and tenomodulin (red). Red arrows point to cells of interest stained red, green arrows point to cells of interest stained green. Samples were counter-stained for nucleus (blue). Data are presented as mean ± SD. * indicated $p < 0.05$. Scale bar = 100 μm.

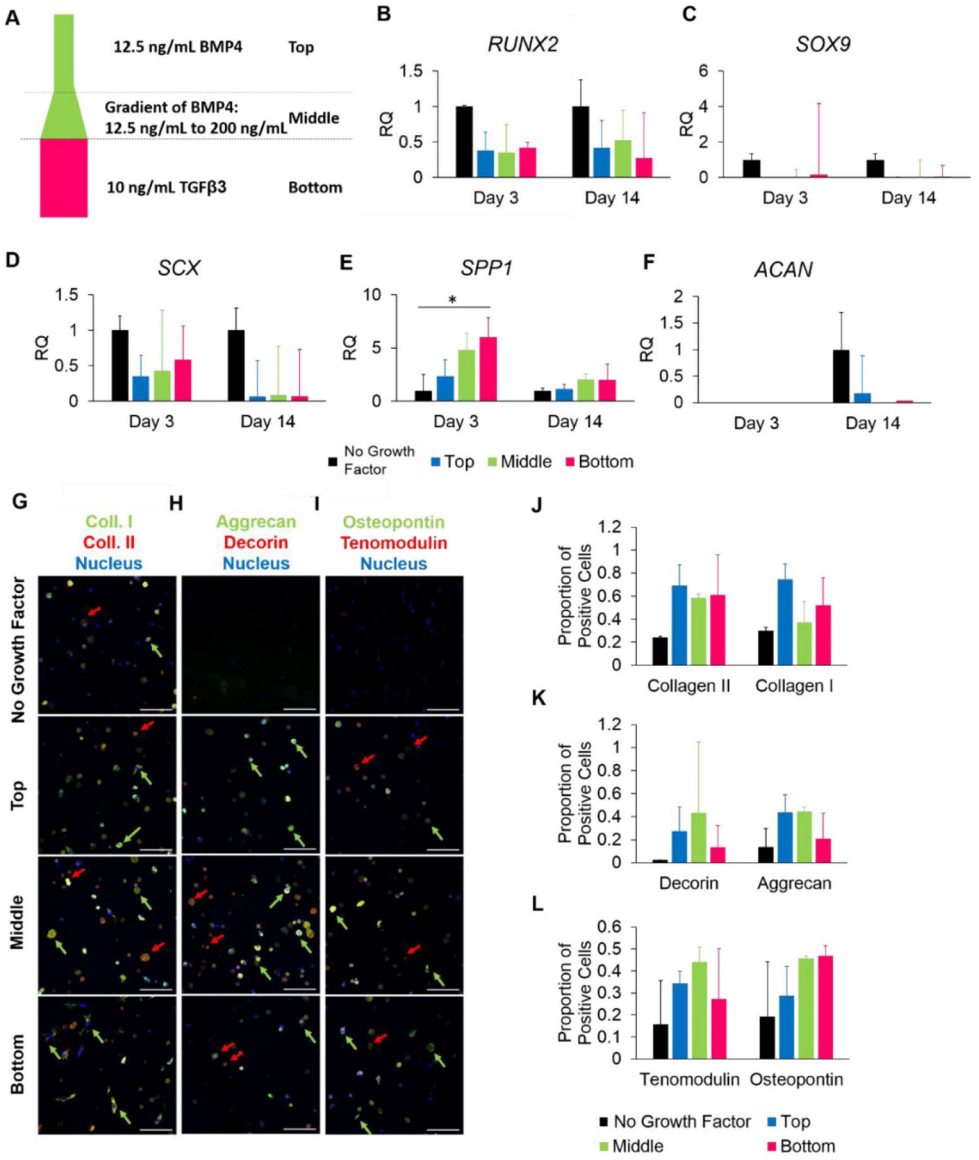

Figure 4.

Effect of spatial differences in growth factor BMP4 and TGFβ3 on MSC gene and protein expression. (a) Schematic of growth factor layout. (b)–(f) Relative expression from cells isolated from the top, middle, and bottom of the construct for (b) *RUNX2*, (c) *SOX9*, (d) Scleraxis, (e) osteopontin, and (f) aggrecan. (g)–(i) Confocal images of immunofluorescence staining for (g) aggrecan (green) and decorin (red), (h) collagen I (green) and collagen II (red), and (i) osteopontin (green) and tenomodulin (red). Red arrows point to cells of interest stained red, green arrows point to cells of interest stained green. Samples were counter-stained for nucleus (blue). (j)–(l) graphs demonstrating proportion of positively labelled cells for (g), (h), and (i), respectively. Data are presented as mean ± SD. * indicated $p < 0.05$. Scale bar = 100 μm.

Table 1.

Layers cast for multiple spatial organizations of protein within GelMA constructs. 100% protein indicates 100% of highest concentration of protein used. 75% Protein A indicates that the hydrogel precursor has a concentration of protein that is 75% of the highest concentration used. For example, fabrication of the single gradient of BMP4 would have layers with protein concentration: layer 1: 200 ng ml^{-1}, layer 2: 150 ng ml^{-1}, layer 3: 100 ng ml^{-1}, layer 4: 50 ng ml^{-1}, layer 5: 0 ng ml^{-1}.

Organization	Layer 1	Layer 2	Layer 3	Layer 4	Layer 5
Distinct phases	100% protein A	100% protein B	—	—	—
Single gradient	100% protein A	75% protein A	50% protein A	25% protein A	0% protein A
Inverse gradient	100% protein A	75% protein A	50% protein A	25% protein A	0% protein A
	0% protein B	25% protein B	50% protein B	75% protein B	100% protein B